24th COBEM - 2017

24th ABCM International Congress of Mechanical Engineering
December 3-8, 2017, Curitiba, PR, Brazil

COBEM-2017-2660
A LOW COMPUTATIONAL COST ANALYSIS FOR A VERTICAL AXIS WIND TURBINE ACCORDING TO MSTM

Ana Carolina Rafael Maia
Hernán Darío Cerón-Muñoz
Sao Carlos School of Engineering, University of Sao Paulo - Avenida Trabalhador Sancarlense, 400 - São Carlos, SP - Brazil
ana.carolina.maia@usp.br, hernan@sc.usp.br

Abstract. *Many countries have been investing in wind energy, due to several benefits such as wide resource availability and low cost. Brazil has a remarkable wind potential and relevant market share in the global energy production, showing large evidence of research done in this field. Vertical-axis wind turbines (VAWTs) could be advantageous to traditional horizontal turbines (HAWTs) because of their less environmental impact and better performance for poor wind conditions, with special small-size applications for urban areas. In this work, a standard roof-top VAWT was chosen for power analysis in the city of São Carlos, based on the Multiple Streamtubes Model (MSTM). The output power obtained is similar to the real data provided by the manufacturer in respect to curve trending, but with variations in scale. MSTM overestimated the real results in about 70%, due to its simplifications and uncertainties in the turbine parameters. However, considering further improvements, this model could be quite useful for an initial analysis at a low computational cost required. Moreover, the selected turbine could supply significant part of the mean local energy consumption, for home or academic purposes.*

Keywords: *wind energy, wind turbine, vertical axis wind turbine (VAWT), computational aerodynamics, multiple streamtubes model (MSTM)*

1. INTRODUCTION

Since economic progress and social welfare are closely related to electricity consumption, energy generation is currently one of the most important discussion topics in the world. The increase in the global demand and the climate changes occurred over the past decades require a smooth transition to a new global energy model based on the use of renewable sources (Martins *et al.*, 2008). Wind energy figures as a promising alternative for sustainable development in the world because of its several advantages to other renewable sources, such as low cost, water independence in production process and meaningful decrease in carbon emissions (GWEC, 2016a).

Currently, the wind industry is present in more than 80 countries, including 28 with at least 1 GW of installed capacity each. In 2015, wind supplied more new power than any other technology, being responsible for 4% of the world's energy production (GWEC, 2016a). Although most of the top 10 wind power suppliers shown in Fig. 1 are developed countries, there has been recently noticeable expansion to other markets around the world, such as Africa, Asia and Latin America.

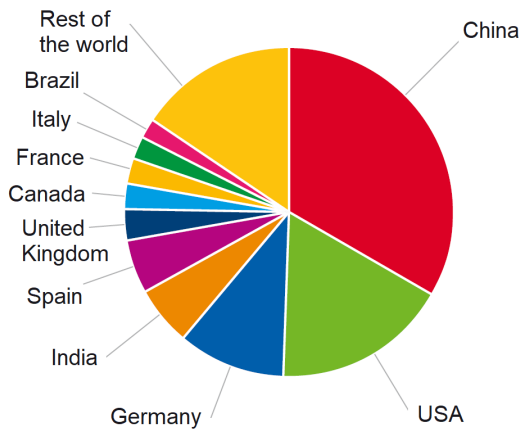

Figure 1. Top 10 cumulative capacity in 2015 (Adapted from GWEC, 2016a)

Brazil has a remarkable wind potential, being considered the most promising onshore market in America Latina until 2020. Despite its recent economic and political woes, the Brazilian wind industry keeps powering ahead. In 2016, Brazil joined the top 10 countries with more than 10 GW of accumulated capacity (GWEC, 2016a). Brazil also ranked fourth position in the world for new installed capacity in 2015, following China, USA and Germany (GWEC, 2016b). Nevertheless, wind is responsible for only 7.1% of the national energy production, led by hydroelectric and biomass as shown in Fig. 2, where SHC is the short term for small hydroelectric centrals.

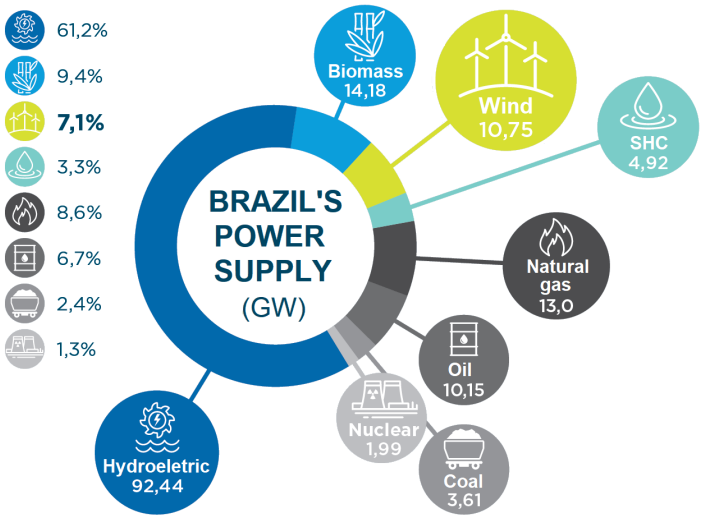

Figure 2. Brazil's Power Supply in 2016 (Adapted from ABEEólica, 2017)

Vertical axis wind turbines (VAWTs) are a developing technology advantageous to the traditional horizontal axis wind turbines (HAWTs), due to their independence of wind direction and lower regime speeds, becoming less noisy and safer for the surrounding environment. However, their complicated aerodynamic modeling makes performance optimization challenging for conventional finite element methods, requiring special tools for predicting its performance.

Recent studies in wind energy trends estimate that within the next three decades, VAWTs can dominate the wind power technology, due to less land space required for same energy production when compared to HAWTs, especially in urban areas (Ishugah *et al.*, 2014). This work dealt with a power generation study on a standard small-size VAWT in the city of São Carlos (Brazil), according to the implementation of the Multiple Streamtubes Model (MSTM).

2. COMPUTATIONAL AERODYNAMICS OF VERTICAL AXIS WIND TURBINES

Wind turbines can be classified according to the orientation of the rotor axis in respect to the ground. There are two main categories: horizontal axis wind turbines (HAWTs) and vertical axis wind turbines (VAWTs). Although the first type has dominated the large-scale market for over 30 years, VAWTs are an innovative technology for small applications (up to 100 kW), especially for urban areas and roof-top mounting (WWEA, 2015; Segupta and Biswas, 2017).

The Multiple Streamtubes Model (MSTM) is one version of the streamtubes models, an approximation for power prediction of VAWTs based on the combination of the Blade Element Method (BEM) and the momentum theory. The resultant methodology is easy to implement and produces reasonable error at low computational cost, when compared to finite element method simulations or vortexes modeling (Vallverdú, 2014). However, this procedure relies on empirical airfoil data such as lift and drag curves as input.

In MSTM, the turbine is represented by an actuator disk with the total area swept by blades and the same thrust during operation. The domain is divided into a finite number of streamtubes parallel to the flow direction. Figure 3 shows a scheme for a VAWT domain with a single blade at an arbitrary angular position in the counterclockwise direction. The origin at the top of the disk splits the domain into front and back half-cycles, which have different flow behaviors. The front half-cycle is responsible for the most energy extraction as directly facing the approaching wind, whereas the back half-cycle experiences less available energy or even returning energy back to the flow (Vallverdú, 2014).

The method's main hypothesis is that all the velocity components perpendicular to the tubes are neglected, setting up a unidirectional problem in the flow direction. Therefore, there must be no mass, momentum or energy transfer between surrounding streamtubes (Vallverdú, 2014).

There are three different flow states during the energy extraction process, represented by the corresponding flow velocities. The free stream flow velocity U_∞ is the approaching wind that has not been disturbed by the turbine yet. The flow velocity at the turbine u is reduced due to its interaction with the actuator disk during operation. The wake flow velocity u_w represents the last stage where the flow has lost the part of its kinetic energy for extraction from the turbine.

An algebraic analysis from momentum theory can demonstrate that the flow velocity at the turbine is the average between the free stream and wake velocities.

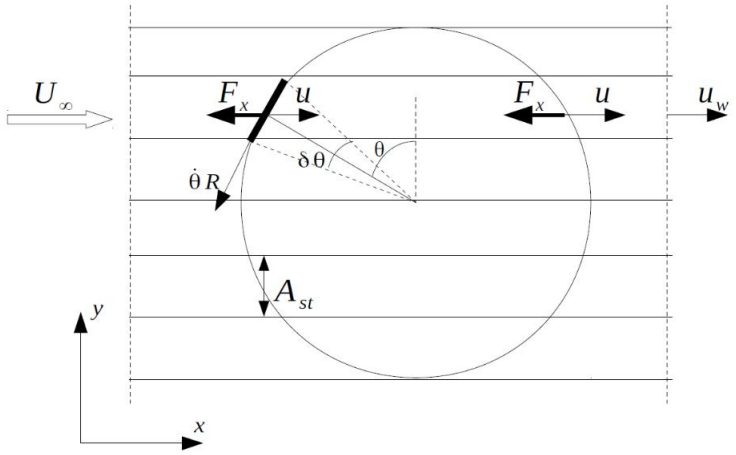

Figure 3. VAWT domain according to MSTM (Adapted from Vallverdú, 2014)

One can notice that for any azimuthal position θ, the wind flow approaches the blade in a different angle, resulting in different angles of attack during one cycle. The blade rotation causes an induced tangential velocity v in the blade in the opposite direction, which magnitude is shown in Eq. (1), where *R* is the turbine radius. The tip-speed ratio *TSR* is a dimensionless parameter to describe the turbine operation as a function of the imposed wind conditions, defined in Eq. (2) as the ratio between the induced and the free stream flow velocity.

$$v = \dot{\theta} R \tag{1}$$

$$TSR = \frac{\dot{\theta} R}{U_\infty} \tag{2}$$

Figure 4 shows the kinematic analysis of a single blade at an arbitrary position. The relative wind flow velocity u_r is resultant from the vector sum of the main velocity components mentioned previously. For any azimuthal position, the relative flow velocity can be expressed as a function of the normal V_n and tangential V_t velocities, according to Eqs. (3), (4) and (5).

$$V_t(\theta) = v + U_\infty \cos\theta \tag{3}$$

$$V_n(\theta) = U_\infty \sin\theta \tag{4}$$

$$u_r(\theta) = \sqrt{V_t^2(\theta) + V_n^2(\theta)} = U_\infty \sqrt{TSR^2 + 2TSR\cos\theta + 1} \tag{5}$$

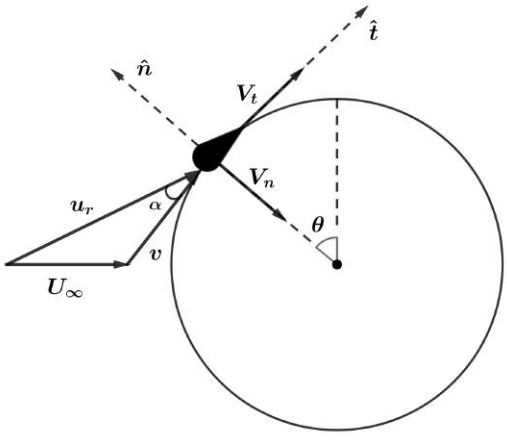

Figure 4. Scheme of the kinematics of one blade

For a sufficiently large number of streamtubes, the tube width may be approximated by the corresponding arc length $\Delta\theta$. Thus, the streamtube area A_{st} is described in Eq. (6), where θ_1 is the middle point of the first tube. In this method, all aerodynamic magnitudes lack one order distance unit because the turbine is approached as a two dimensional problem (Vallverdú, 2014).

$$A_{st} = R\Delta\theta \sin\theta_1 \tag{6}$$

The flight path angle β is defined as the angle between the airfoil chord c and the horizontal axis, described in Eq. (7). This parameter is important to represent the horizontal component of each aerodynamic quantity that will compute the thrust force parallel to the streamtubes. The angle of attack α is derived from the kinematic analysis in Eq. (8). However, Vallverdú (2014) suggests its calculation for implementation as shown in Eq. (9).

$$\beta(\theta) = \tan^{-1}\left(\frac{TSR\sin\theta}{\frac{u}{U_\infty} + TSR\cos\theta}\right) \tag{7}$$

$$\alpha(\theta) = \tan^{-1}\frac{V_n}{V_t} = \tan^{-1}\left(\frac{\sin\theta}{\cos\theta + TSR}\right) \tag{8}$$

$$\alpha(\theta) = mod\Big(\frac{\pi + \beta - \theta}{2\pi}\Big) - \pi \tag{9}$$

Each governing equation of fluid dynamics can be applied in its integral form to each streamtube domain. Equations (10), (11) and (12) describe the conservation of mass, momentum and energy, respectively, where $\dot{m}$ is the mass flow, ρ is the air density, and F_x is the net force parallel to the streamtubes.

$$\dot{m} = \rho u A \tag{10}$$

$$\dot{m}(u_w - U_\infty) = -F_x \tag{11}$$

$$\frac{1}{2}\dot{m}(u_w^2 - U_\infty^2) = -F_x u \tag{12}$$

The interference factor λ is a measure of the reduction in the flow velocity at the turbine, caused by the disturbance from the presence of the blades. In MSTM, each streamtube has its own interference factor, as defined in Eq. (13). Using this definition with Eqs. (10), (11) and (12), the actual flow velocity at the turbine can be evaluated from Eq. (14).

$$\lambda = \frac{u}{U_\infty} \tag{13}$$

$$u = U_\infty(2\lambda - 1) \tag{14}$$

The resultant thrust force in each streamtube C_{fx} is defined in Eq. (15) as a fraction of the maximum that would be obtained without any speed reduction in the flow. The thrust force coefficient from momentum theory $C_{fx,m}$ presented in Eq. (16) is calculated by combining the interference factor and the governing equations. However, Glauert (1935) proposed a linear correction for lower interference factors described in Eq. (17), in order to improve the method's suitability at these conditions, which are common for higher values of *TSR*.

$$C_{fx} = \frac{F_x}{\frac{1}{2}\rho A_{st} U_\infty^2} \tag{15}$$

$$C_{fx,m} = 4\lambda(1-\lambda), \lambda \geq 43/60 \tag{16}$$

$$C_{fx,m} = \frac{1849}{900} - \frac{26}{15}\lambda, \lambda < 43/60 \tag{17}$$

Figure 5 presents the aerodynamics of a single blade at an arbitrary position, where L is the lift and D is the drag forces, described in Eq. (18) and Eq. (19), respectively (Vallverdú, 2014). The resultant thrust force exerted on the blade F is calculated from a load analysis of the aerodynamic forces in the flow direction, according to Eq. (20). The horizontal component of the thrust force F_x is shown in Eq. (21), in terms of the lift C_l and drag C_d coefficients. The *x* and *y* directions of the domain are represented by the unit vectors $\hat{i}$ and $\hat{j}$, respectively.

$$L = \frac{1}{2}C_l\rho c u_r^2 \tag{18}$$

$$D = \frac{1}{2}C_d\rho c u_r^2 \tag{19}$$

$$\mathbf{F}(\theta) = (D\cos\beta - L\sin\beta)\hat{\mathbf{i}} + (D\sin\beta + L\cos\beta)\hat{\mathbf{j}} \tag{20}$$

$$F_x(\theta) = \frac{1}{2}\rho c u_r^2(C_d\cos\beta - C_l\sin\beta) \tag{21}$$

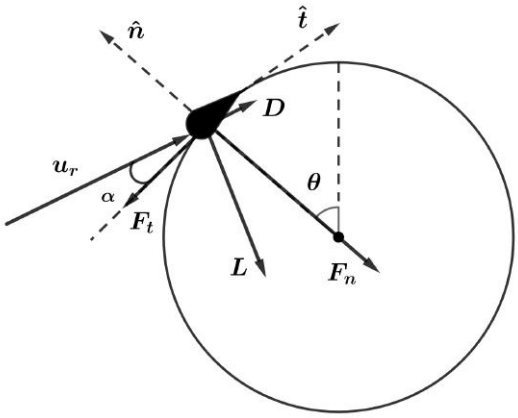

Figure 5. Scheme of the aerodynamics of one blade

In order to obtain the mean horizontal thrust force in each streamtube $F_{x,st}$, the horizontal thrust force from load analysis is integrated over a full cycle in Eq. (22), considering the number of blades n. This integral can be solved with a first order approximation of Taylor series (Vallverdú, 2014). The turbine solidity σ is introduced in Eq. (23), defined as the ratio between the sum of the chord length of all the blades over the turbine diameter. Hence, the thrust force coefficient from load analysis $C_{fx,l}$ is described in Eq. (24), where θ_m is the mean coordinate of the selected streamtube.

$$F_{x,st} = \frac{n}{2\pi}\int_{\theta_m-\Delta\theta/2}^{\theta_m+\Delta\theta/2} F_x(\theta)d\theta = \frac{n\Delta\theta}{2\pi}F_x(\theta_m) \tag{22}$$

$$\sigma = \frac{nc}{2R} \tag{23}$$

$$C_{fx,l}(\theta) = \frac{\sigma}{\pi\sin\theta_1}\frac{u_r^2}{U_\infty^2}(C_d\cos\beta - C_l\sin\beta) \tag{24}$$

The convergence of the streamtubes models such as MSTM consists in coupling Eq. (16) or Eq. (17) and Eq. (24) obtained for the thrust force coefficient from both methods, in order to find the solution for the interference factor of each tube. Thus, the flow velocity at the turbine can be recalculated from Eq. (14), as well as all the other dependent variables.

The instantaneous torque T_b produced by each blade is calculated from the total force exerted by the wind on the blades in Eq. (25). It is described by the corresponding torque coefficient $C_{t,b}$ in Eq. (26) for any position (Vallverdú, 2014). Since the orientation of the aerodynamic forces varies with the azimuthal position, the lift $\hat{l}$, drag $\hat{d}$ and torque $\hat{t}$ unit vectors are introduced in Eqs. (27) through (29), respectively.

$$\mathbf{T_b}(\theta) = RF(\theta).\hat{\mathbf{t}} = R(L\hat{l} + D\hat{d}).\hat{\mathbf{t}} \tag{25}$$

$$C_{t,b}(\theta) = \frac{T_b(\theta)}{\frac{1}{2}\rho c U_\infty^2 R} \tag{26}$$

$$\hat{\mathbf{l}} = -\sin\beta\hat{\mathbf{i}} + \cos\beta\hat{\mathbf{j}} \tag{27}$$

$$\hat{\mathbf{d}} = \cos\beta\hat{\mathbf{i}} + \sin\beta\hat{\mathbf{j}} \tag{28}$$

$$\hat{\mathbf{t}} = -\cos\beta\hat{\mathbf{i}} - \sin\beta\hat{\mathbf{j}} \tag{29}$$

For turbines with equidistant blades, the instantaneous torque coefficient obtained by all blades C_t is described in Eq. (30). In MSTM, each one of the blades will produce the same torque profile, but with a phase different of $2\pi/n$, resulting in a torque curve with this periodicity (Vallverdú, 2014).

$$C_t(\theta) = \frac{\sigma}{n}\sum_{i=1}^{n} C_{t,b_i}\left(\theta + \frac{i-1}{n}2\pi\right) \tag{30}$$

The VAWT's output power coefficient C_p is calculated in Eq. (31) through the sum of the mean instantaneous power in front and back half-cycles $C_{p,f}$ and $C_{p,b}$, respectively. Both coefficients are identical due to the symmetry proposed by

MSTM, as shown in Eq. (32). The wind flow area is defined for the power calculation in Eq. (33), where h is the blade wingspan. Finally, the output power P is calculated through Eq. (34).

$$C_p = C_{p,f} + C_{p,b} \tag{31}$$

$$C_{p,f} = C_{p,b} = \frac{\sigma TSR}{2\pi} \int_0^{\pi} C_{Tb}(\theta) d\theta \tag{32}$$

$$A = 2Rh \tag{33}$$

$$P = C_p \frac{1}{2} \rho U_{\infty}^3 A \tag{34}$$

The characteristic curve of a VAWT is the output power coefficient against the tip-speed ratio, for the cases of constant or variable blade rotation speed. Wind tunnel experiments show that there may be an optimal value of TSR responsible for the maximum power coefficient (Sheldahl and Klimas, 1981). Hence, a VAWT should be designed with a control system to operate at the optimal *TSR* and provide the best possible exploitation of the local wind resource.

3. Methodology

A code for VAWT modeling and power analysis was developed on MATLAB, based on the implementation of MSTM. The code structure is divided into two main parts: interference factor evaluation and power calculation. For the first part, an initial guess of unity is made for the interference factor and then results are calculated for each 0.001 decrement until reaching 0.5. The value that gives the least relative error between experimental and theoretical thrust force coefficients is chosen as solution for the interference factor. Note that according to Eq. (14), values below 0.5 would give negative values for the flow velocity.

The VAWT installation takes place on campus 2 from Universidade de São Paulo at São Carlos, due to the suitable open area and intense research activities. The city is considered an important industrial and research center in the countryside of the state of São Paulo, with its local economy focused on agriculture, industry and academia (IBGE, 2017). The Brazilian Atlas of Wind Potential also confirms good meteorological conditions in the countryside of the state of São Paulo (Amarante *et al.*, 2001).

Local geographic coordinates were obtained by Google Maps and plugged into the online wind data service based on the Brazilian Wind Atlas (CRESESB, 2014). The obtained mean annual wind data from a 50-meter reference height in a Weibull distribution was converted into the rotor height, considering a 20-meter building plus the turbine height (7.8 m).

The site satellite view in Fig. 6 shows a plain terrain, with occasional trees and buildings. According to the European Wind Atlas, the surface of the installation site may be classified as 2 in the corresponding scale. Suggested surface rugosity z_0 for these conditions is 3 cm (Dutra, 2008). The wind velocity profile at the rotor was obtained through the logarithmic model for the geotropic boundary layer shown in Eq. (35), where k_0 is the Vón Karmán constant, v^* is the friction wind speed and z is the rotor height (Montezano, 2012).

$$V(z) = \frac{1}{k_0} v^* \ln\left(\frac{z}{z_0}\right) \tag{35}$$

Figure 6. Satellite view for USP São Carlos (Google Maps, 2017)

For the turbine selection, only the H rotor type was considered. Its geometry of straight blades makes this design the simplest for prototyping and manufacturing. In addition, this is the most suitable kind for the hypothesis of constant rotor

diameter imposed by MSTM. Several standard small size VAWTs were compared, including the manufacturers from the Small Wind Report (WWEA, 2015). The main criteria was low cut-in wind speed to have a compatible exploitation of the velocities observed at the installation site. Besides, nominal power per mass were considered, whereas all turbines analyzed had close noise levels.

For this analysis, Aeolos – V 3 kW (Fig. 7) was selected, which is the manufacturer's roof-top version with the highest power available (Aeolos Wind Energy, 2017). The available turbine parameters are shown in Tab. 1. Since no information for airfoil dimensions was given, NACA 0012 was assumed as one of recommended profiles for vertical turbines. The airfoil's characteristic curves were obtained from wind tests from Sandia National Laboratories (Sheldahl and Klimas, 1981). The remaining airfoil parameters were assumed from the proportion in respect to the specified dimensions.

Table 1. Aeolos – V 3 kW parameters (Aeolos Wind Energy, 2017)

Number of blades	n	3
Airfoil chord (1)	c	0,7 m
Blade wingspan (1)	h	8,4 m
Rotor diameter	d	3 m
Tower height	H	6 m
Cut-in wind speed	V_i	1.5 m/s
Rated wind speed	V_r	11 m/s
Survival wind speed	V_s	52.5 m/s
Generator efficiency	η	96 %

(1) not specified by the manufacturer

Figure 7. Turbine Aeolos V – 3 kW (Adapted from Aeolos, 2017)

The air properties were taken according to standard temperature and pressure conditions for the city of São Carlos, considering its mean altitude of 859 m plus the turbine height (INMET, 2017; Kroo, I., 1997). The Reynolds number was calculated from the nominal speed as a median value, whereas the acting wind speeds at São Carlos are lower. Table 2 show the air flow properties used in this analysis.

Table 2. Air flow properties (Kroo, 1997)

Density	ρ	1.124 kg/m^3
Dynamic viscosity	η_{air}	1.761×10^{-5} Ns/m^2
Reynolds number	*Re*	1.4×10^5

The available airfoil database for a closer value of Reynolds number (1.5×10^5) was assumed. In this condition, the critical angle of attack for stall is approximately $10°$. Since the input angles of attack in the database were all integers,

the increment for the azimuthal angle was defined as 1°. For this analysis, the number of streamtubes was set to 100, the double of the assumption made on existing literature (Vallverdú, 2014). Furthermore, the generator efficiency was also computed for the power calculation.

4. RESULTS AND DISCUSSION

The annual wind speed distribution for the installation place is shown as a histogram in Fig. 8. Wind speeds below the cut-in limit (1.5 m/s) were neglected since no energy is produced at these conditions. The mean local wind speed is estimated in 5.6 m/s, quite lower than the turbine nominal wind speed (11 m/s). Only the significant wind speed range of the site was considered in analysis (between 2 and 15 m/s).

Since no information about an optimal tip-speed ratio or any correlation between the operational parameters was available, the solution was to assume a range of 1-2.5 for the tip-speed ratio, typical for BEM operation (Vallverdú, 2014). For 15 increments of *TSR* decreasing with wind speed, the resultant rotation profile increases almost linearly with wind speed until it reaches a maximum near the rated speed. Moreover, all values are kept below one third of maximum rotation speed (320 rpm), considering operating wind speeds much lower than cut off speed (52.5 m/s).

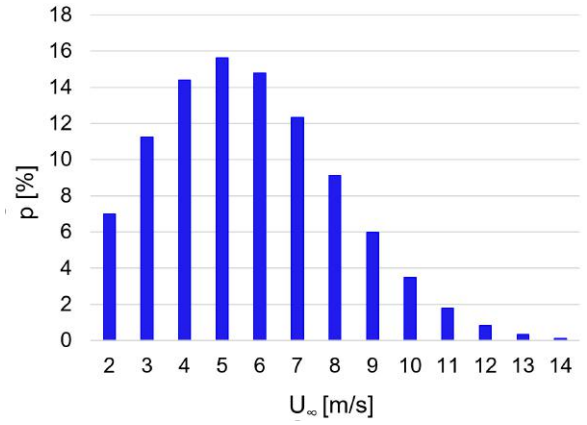

Figure 8. Wind speed probability density at the rotor height

The output power curve as a function of wind speed is presented in Fig. 9. The comparison with the real results provided by the manufacturer shows that the curves are quite similar in tendency with variations in scale. One can notice that power obviously increases with wind speed, as expected from more energy available in the wind. The MSTM results overestimated the real ones without reaching a maximum power value. The relative error decreases with wind speed, being approximately 70% for median values.

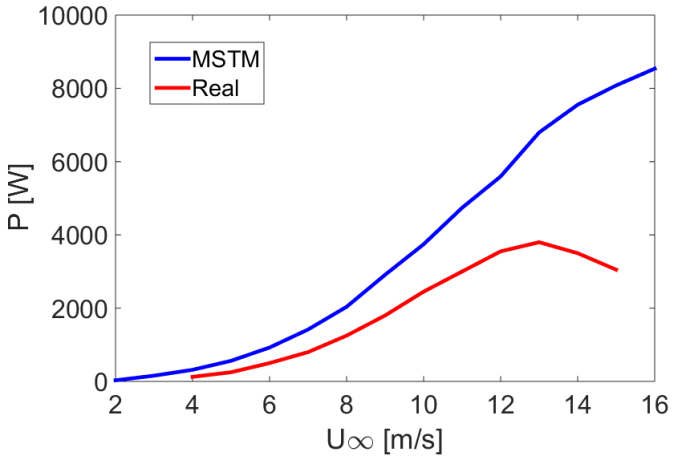

Figure 9. Power curves for turbine Aeolos – V 3 kW

The manufacturer's brochure additionally provides an estimate for the annual energy generation as a function of the wind speed. For the mean velocity of site (5.6 m/s), an interpolation of the real data gives a value of 6820 kWh. Considering the local resource assessment, the local annual energy production is estimated by MSTM in 9000 kWh. The annual energy consumption of São Carlos in 2016 is 878.5 TWh for 243,756 inhabitants, resulting in an annual

consumption per capita of 3603.5 kWh (Governo do Estado de São Paulo, 2017; IBGE, 2017).

The criteria to evaluate the computational cost of the analysis was the total time spent on simulation, which was 20 minutes. Existing literature suggests several minutes for a double MSTM with half of the number of streamtubes defined previously (Vallverdú, 2014). However, according to the Matlab time review, most of the time was spent only for airfoil data acquisition and interpolation.

5. CONCLUSION

Wind energy figures as a competitive technology for electricity generation, due to resource availability, low energy cost and low environmental impact. Recent studies have shown the current favorable situation of the global wind market with expansion to developing countries. Besides its remarkable wind potential, Brazil has an expressive market share in the global energy production that shows large evidence of research done in this field.

VAWTs are an advantageous solution for urban energy generation, because of their better performance at poor wind conditions and less disturbance in the installation site. Considering only the mean local energy consumption, the turbine Aeolos V – 3 kW could supply partially a 3-people household in the city of São Carlos. Nonetheless, one should investigate economic, political and environmental aspects for a complete feasibility analysis of this turbine at the desired site.

Streamtube models like MSTM can overcome the challenge in aerodynamic modeling of VAWTs with traditional methods such as finite elements. Considering further improvements, MSTM can provide satisfactory results with low computational cost, being quite useful for an initial power analysis. The main advantages of this method are simplicity in implementation and fast simulation time, requiring only basic programming skills.

Adopted criteria in this analysis was sufficient to produce accurate results comparable to the real data. However, similar trends with variation in scale indicates primarily that power losses have not been properly computed. The significant difference in power magnitude might be associated to the model hypothesis, especially about the symmetry in front and back half-cycles imposed by MSTM. In addition, the uncertainties in the turbine geometric and operational parameters strictly compromise the precision of the power results.

The MSTM results overestimated the real output power in approximately 70% for mean wind speed values. The annual energy estimative from local annual statistical distribution was likewise higher than real data. Although most papers published so far in this field deals with modified DMST models, it should be clear that MSTM was chosen here for an initial test version. Before validating the simplest version with only one actuator disk, the computational model cannot be improved.

Future work consists in the implementation of a DSTM for representing the back half-cycle behavior. Existing methods in literature could be used for corrections to effects such as dynamic stall, wake interaction and blade tip losses. Evaluation of Reynolds number for each case could improve the airfoil data acquisition accounting for variations in aerodynamic forces due to wind speed changes. Since the manufacturer's data does not specify all operational conditions, a better validation involves wind tunnel tests with a H rotor prototype with all properties evaluated. Moreover, modifications in the code structure could make it easier for the user to manage the input data.

6. ACKNOWLEDGEMENTS

This work was supported by the Fluid Dynamics Research Center at Illinois Institute of Technology (IIT) during the Summer Immersion Research Program 2016 sponsored by International Institute of Education (IIE) and Coordenação de Aperfeiçoamento de Pessoal de Nível Superior (CAPES).

7. REFERENCES

Aeolos Wind Energy, 2017. "Aeolos - V 3 kW Brochure".

Amarante, O.A., Brower, M., Zack, J., Eolica, C.S.E. and Solutions, T., 2001. "Atlas do Potencial Eólico Brasileiro". In *Atlas do Potencial Eólico Brasileiro*, Ministerio de Minas e Energia Eletrobras.

CRESESB, 2014. "Potencial Eólico - Atlas do Potencial Eólico Brasileiro". Available at: <http://www.cresesb.cepel.br>. Acessed on September 23, 2017.

Dutra, R., 2008. "Energia eólica: Princípios e tecnologia". *Rio de Janeiro: Centro de Referência para Energia Solar e Eólica Sérgio de Salvo Britto*.

Glauert, H., 1935. "Airplane propellers". In *Aerodynamic theory*, Springer, pp. 169–360.

Governo do Estado de São Paulo, 2017. "Anuário de energéticos por município - Estado de São Paulo". Available at: <http://dadosenergeticos.energia.sp.gov.br/portalcev2/intranet/BiblioVirtual/diversos/anuario_energetico_municipio.pdf>. Acessed on September 25, 2017.

GWEC, 2016a. "Global Energy Outlook 2016".

GWEC, 2016b. "Global Wind Report 2015: Annual Market update".

IBGE, 2017. "IBGE Cidades: Brasil/São Paulo/São Carlos". Available at: <https://cidades.ibge.gov.br/v4/brasil/sp/sao-carlos/panorama>. Acessed on September 23, 2017.

INMET, 2017. "Estações Automáticas". Available at: <http://www.inmet.gov.br/portal/index.php?r=estacoes/estacoesautomaticas>. Acessed on September 24, 2017.

Ishugah, T., Li, Y., Wang, R. and Kiplagat, J., 2014. "Advances in wind energy resource exploitation in urban environment: A review". *Renewable and Sustainable Energy Reviews*, Vol. 37, pp. 613–626.

Kroo, I., 1997. "Standard Atmosphere Computations". Available at: <http://aero.stanford.edu/stdatm.html>. Acessed on September 25, 2017.

Martins, F., Guarnieri, R. and Pereira, E., 2008. "O aproveitamento da energia eólica". *Revista Brasileira de Ensino de Física*, Vol. 30, No. 1, p. 1304.

Montezano, B.E.M., 2012. *Estratégias para identificação de sítios eólicos promissores usando Sistema de Informação Geográfica e Algoritmos Evolutivos*. Ph.D. thesis, Universidade Federal do Rio de Janeiro.

Segupta, A.R. and Biswas, A., 2017. "Vertical Axis Wind Turbines in the Built Environment - A Review". *Renewable and Sustainable Energy Reviews*.

Sheldahl, R.E. and Klimas, P.C., 1981. "Aerodynamic characteristics of seven symmetrical airfoil sections through 180-degree angle of attack for use in aerodynamic analysis of vertical axis wind turbines". Technical report, Sandia National Laboratories.

Vallverdú, D., 2014. *Study on vertical-axis wind turbines using streamtube and dynamic stall models*. Ph.D. thesis, Illinois Institute of Technology.

WWEA, 2015. "2015 Small Wind World Report Summary".

8. RESPONSIBILITY NOTICE

The authors are the only responsible for the printed material included in this paper.